HGG Advances

BRIEF COMMUNICATION

Homozygous variants in *EIF3K* associated with neurodevelopmental delay, microcephaly, and growth retardation

Bobbi McGivern,[1,11,12,*] Tess Holling,[2,11] Maria J. Guillen Sacoto,[1] Hákon Gudbjartsson,[1] Ibrahim M. Abdelrazek,[3] Malik Alawi,[4] Yan Bai,[1] Olaf Bodamer,[5,6] Amy Crunk,[1] Amy E. Dameron,[1] Lisa M. Dyer,[1] Lindsay B. Henderson,[1] Mira Irons,[5,7] Kerstin Kutsche,[2,8] Caroline McGowan,[5] Kristin G. Monaghan,[1] Kaitlyn O'Connor,[9,10] Asma Rashid,[5] Olivia L. Redlich,[1] Adi Reich,[1] Christopher Simotas,[9,10] Sara Welner,[9,10] and Ingrid M. Wentzensen[1]

Summary

We report two rare homozygous variants, including a recurrent missense and intronic variant, in the *EIF3K* gene in four unrelated individuals with global developmental delay, microcephaly, proportionate short stature, dysmorphic craniofacial features, digit flexion deformities, and the cardiac anomaly, patent ductus arteriosus. Three individuals, who were all of Puerto Rican descent, were homozygous for the NM_013234.3:c.128A>G; p.(Asp43Gly) variant in *EIF3K* and homozygous for a missense variant in *SYNE4* (NM_001039876.2:c.355C>T; p.(Arg119Trp)). *SYNE4* is associated with autosomal recessive bilateral sensorineural hearing loss, which was also reported in these probands. Analysis of our dataset confirmed these *EIF3K* and *SYNE4* variants were in linkage disequilibrium in affected individuals, suggesting a possible common ancestor and founder event. A fourth individual from Egypt harbored the homozygous intronic variant c.355-13A>G in *EIF3K*, which segregated with the phenotype in the family and led to aberrant splicing of *EIF3K* pre-mRNAs, as shown by insertion of 12 intronic base pairs, skipping of 2 exons, and significantly reduced EIF3K protein levels in skin fibroblasts. Through genetic and functional approaches, we suggest that biallelic *EIF3K* variants are associated with an autosomal recessive syndromic neurodevelopmental disorder with growth retardation, microcephaly, congenital heart defect, and other anomalies.

Introduction

Eukaryotic translation initiation factor 3 (eIF3) is the largest of the eukaryotic initiation factors, containing 13 subunits important for coordinating the assembly of the 43S pre-initiation complex.[1,2] The function of the smallest subunit, eIF3k, is not well defined, but it might serve as a structural scaffold with surfaces for binding to other eIF3 subunits and to RNA itself.[3] Although eIF3k is not essential for the assembly of the active mammalian eIF3 complex,[4] it is expected to play a regulatory role as suggested by its conservation in higher organisms and ubiquitous expression in human tissues. Multiple studies propose that eIF3k might have a role in autophagy,[5] endoplasmic reticulum stress,[6] cellular aging, and/or apoptosis.[7]

Clinical reports of individuals with variants in the *EIF3K* gene are limited.[8,9] Several *de novo* heterozygous variants were reported from large cohorts of individuals with autism spectrum disorder.[10,11] To our knowledge, no individuals with biallelic *EIF3K* variants have been reported.

Here, we describe case-level details of three unrelated Puerto Rican individuals with a syndromic neurodevelopmental phenotype, hearing impairment, and recurrent homozygous missense variants in *EIF3K* and *SYNE4,* which were shown to be in linkage disequilibrium (LD) in affected individuals in our dataset. Biallelic loss-of-function variants in *SYNE4* are associated with nonsyndromic autosomal recessive hearing loss reported as progressive and high frequency, with onset before early childhood (MIM: 615535). We report significantly overlapping phenotypic information for a fourth individual from Egypt with a homozygous intronic variant in *EIF3K*. Functional fibroblast studies showed altered *EIF3K* pre-mRNA splicing and significantly reduced EIF3K protein levels. Collectively, our data provide promising evidence for *EIF3K* as a novel disease gene for an autosomal recessive neurodevelopmental disorder.

[1]GeneDx, LLC, Gaithersburg, MD 20877, USA; [2]Institute of Human Genetics, University Medical Center Hamburg-Eppendorf, Hamburg, Germany; [3]Department of Human Genetics, Medical Research Institute, Alexandria University, Alexandria, Egypt; [4]Bioinformatics Core, University Medical Center Hamburg-Eppendorf, Hamburg, Germany; [5]Department of Pediatrics, Division of Genetics and Genomics, Boston Children's Hospital, Boston, MA 02115, USA; [6]Broad Institute of Harvard University and MIT, Cambridge, MA 02142, USA; [7]Harvard Medical School, Boston, MA 02115, USA; [8]German Center for Child and Adolescent Health (DZKJ), partner site Hamburg, Hamburg, Germany; [9]Department of Pediatrics, Division of Medical Genetics, Rutgers Robert Wood Johnson Medical School, New Brunswick, NJ 08901, USA; [10]Child Health Institute of New Jersey at Rutgers University, New Brunswick, NJ 08901 USA
[11]These authors contributed equally
[12]Lead contact
*Correspondence: genematcher@genedx.com
https://doi.org/10.1016/j.xhgg.2025.100438.

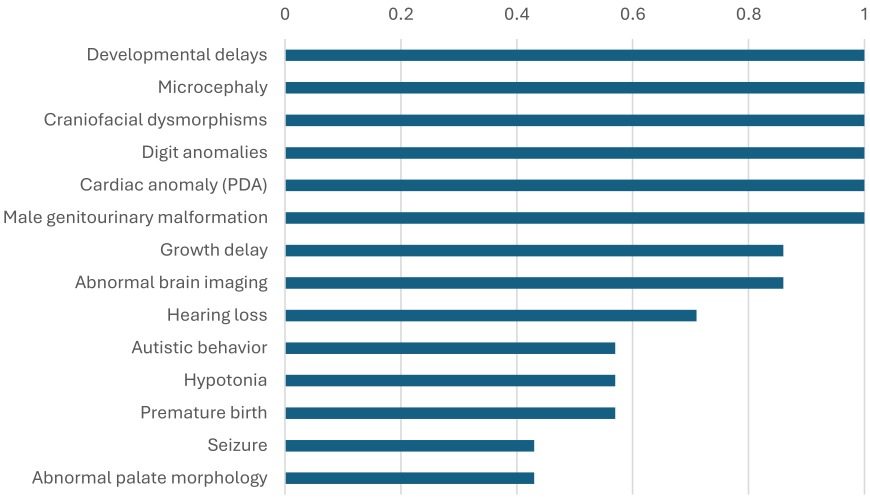

Figure 1. Aggregate clinical findings reported in individuals homozygous for variants in *EIF3K*

Data from individuals 1–4 and <5 additional Puerto Rican individuals identified in the GeneDx genome/exome database who were homozygous for the recurrent missense variant c.128A>G in *EIF3K* and c.355C>T in *SYNE4*. The X axis is the proportion of individuals with each clinical finding reported. For individuals who were not available for consent to case-level inclusion in the study, clinical information is based solely on the information provided at the time of genetic testing.

Subjects, material, and methods

The study was conducted under GeneDx protocol *Research to Expand the Understanding of Genetic Variants: Clinical and Genetic Correlations*, in accordance with the Western Institutional Review Board (WIRB) (protocol 20171030). Individuals not available to consent for case-level publication were presented as aggregate data under GeneDx WIRB protocol 20162523, which states that this research meets the requirements for waiver of consent. Genetic studies for individual 4 were performed as approved by the Ethics Committee of the Hamburg Medical Chamber (PV7038-4438-BO-ff; Hamburg, Germany). The parents of individual 4 provided written informed consent for study participation, clinical data, sample collection, genetic analysis, and publication of results, including publication of photographs (see supplemental methods).

Results

Within GeneDx's database of over 665,000 individuals with genome/exome sequencing (ES), we identified multiple individuals (<10) with similar phenotypes and the same seemingly recurrent homozygous missense variants c.128A>G; p.(Asp43Gly) in *EIF3K* and c.355C>T; p.(Arg119Trp) in *SYNE4* (Table S1). These unrelated individuals, all of whom were of Puerto Rican descent, had no other causative genetic findings and had overlapping phenotypes, including neurodevelopmental delay, microcephaly, short stature, dysmorphic craniofacial features, congenital anomalies, and hearing loss. Three of the fewer than 10 individuals (individuals 1–3) consented to case-level study participation, and their clinical findings are summarized in Figure 1 and Table 1. Other individuals (<5) with these variants who were not available for case-level consent are summarized in aggregate (Figure 1).

Although clinically classified as a variant of uncertain significance (VUS), various *in silico* models (queried on a research basis) support the potential pathogenicity of the rare *EIF3K* c.128A>G missense variant (Table S1). It occurs in the proteasome component (PCI) domain of EIF3K, which mediates and stabilizes protein-protein interactions (UniProt). There are mixed *in silico* predictions for the potential pathogenicity of the *SYNE4* c.355C>T missense variant (Table S1). Our analysis showed LD for these variants within affected population groups in internal GeneDx ES/genome sequencing data as shown by normalized LD values (Table S2).

Through GeneMatcher,[12] individual 4 was identified with a homozygous intronic variant c.355-13A>G in *EIF3K* (Table S1). Sanger sequencing showed both parents and a healthy sibling to be heterozygous carriers (Figure S1A). For the c.355-13A>G variant, splice site prediction programs predicted loss or weakening of the downstream splice acceptor site in intron 4; one program predicted the creation of a new splice acceptor site (Table S1). The phenotype was similar to that of the other individuals and included global developmental delay, growth retardation, dysmorphic craniofacial features, congenital heart defect, and abnormal external genitalia morphology (Figure 1; Table 1).

To analyze whether the *EIF3K* c.355-13A>G variant affected splicing of *EIF3K* pre-mRNAs, we cultivated primary fibroblasts from a skin biopsy of individual 4 and confirmed the homozygous *EIF3K* variant in fibroblast-derived DNA (Figure S1B). Next, we performed *EIF3K* transcript analysis. The RT-PCR product amplified from control cells had the expected size (273 bp) (Figure 2A) and reference sequence (Figure S1C). A larger and a smaller product were amplified from individual 4 cells (Figure 2A). After cloning amplicons from individual 4, we analyzed 51 clones. In 27 clones, we detected an insertion of the last 12 bp of intron 4 between exons 4 and 5 (r.354_355ins355-12_355-1), which is predicted to lead to an insertion of 4 amino acid residues [p.(Trp118_Gln119insPheProSerGln)] (Figure 2B). Nineteen clones contained the reference sequence (Figure 2B). In 5 clones, exon 4 was directly spliced to exon 7, leading to the loss of 145 bp (r.355_499del), which

Table 1. Clinical details of individuals 1–4 with homozygous *EIF3K* variants who consented to case-level publication

	Individual 1	Individual 2	Individual 3	Individual 4
Current age, years	7	11	19	2 years, 6 months
Sex	female	female	female	male
Descent	Puerto Rican	Puerto Rican	Puerto Rican	Egyptian
ES	trio	duo with mother	duo with mother	trio plus variant segregation in two healthy siblings
Additional exome findings	*de novo* copy number gain at 16p11.2 (MIM: 611913)	*MYO15A* NM_016239.3: c.9620G>A, heterozygous, maternally inherited, likely pathogenic variant, consistent with carrier for AR *DFNB3* nonsyndromic hearing loss (MIM: 602666)	none	*SIPA1L3*, NM_015073.3: c.4984+6dup, homozygous, VUS, associated with congenital cataract-45 (MIM: 616851)
Additional genetic testing	negative *CHD7* (MIM: 214800), 625 kb microduplication from 16p11.2 found on chromosomal microarray	normal karyotype, microarray, *GJB2* (MIM: 220290), *MECP2* (MIM: 312750), *FMR1* (MIM: 309550), mitochondrial genome, and negative DNA methylation for Angelman and Prader-Willi (MIM: 105830)	normal karyotype, chromosomal microarray, negative *FMR1* (MIM: 309550), and multi-gene panels for hearing loss and X-linked intellectual disability	normal karyotype
Neurodevelopmental findings				
Delayed speech and language development* (HP: 0000750)	absent speech (HP: 0001344)	absent speech (HP: 0001344)	absent speech (HP: 0001344)	X
Global developmental delay* (HP: 0001263)	X	X	X	X
Delayed gross motor development* (HP: 0002194)	X	X		X
Autism (HP: 0000717)	X	X		
Brain imaging abnormality* (HP: 0410263)	abnormality of cranium shape (HP: 0000267), hypoplasia of the pons (HP: 0012110), hypoplasia of the olfactory tract (HP: 0007036), reduced cerebral white matter volume (HP: 0034295), hyperintensity of cerebral white matter on MRI (HP: 0030890)	ventriculomegaly (HP: 0002119)	thin corpus callosum (HP: 0033725), abnormal cochlea morphology (HP: 0000375)	
ADHD (HP: 0007018)		X	X	
Intellectual disability (HP: 0001249)		X	X	
Atypical behavior (HP: 0000708)		self-injurious behavior (HP: 0100716)	behavioral outbursts (HP: 0000708)	

(*Continued on next page*)

Table 1. ***Continued***

	Individual 1	Individual 2	Individual 3	Individual 4
Seizure* (HP: 0001250)			status epilepticus (HP: 0002133)	
Congenital anomalies				
PDA* (HP: 0001643)	X	X	X	X
Severe to profound B-SNHL* (HP: 0008619)	diagnosed at younger than age 1 year	diagnosed as a newborn	diagnosed at age 2 years (initially left sided but progressed to bilateral)	
Abnormal digit morphology* (HP: 0011297)	camptodactyly (HP: 0012385), adducted thumb (HP: 0001181)	overlapping toe (bilateral) (HP: 0001845)	joint contracture of the 5th finger (HP: 0009183), small toe (HP: 0030031)	camptodactyly of 2nd–5th fingers (HP: 0001215), overlapping toe (bilateral) (HP: 0001845), hypoplastic toenails (HP: 0001800)
Abnormal palate morphology (HP: 0000174)	submucous cleft palate (HP: 5201016)		high palate (HP: 0000218)	high palate (HP: 0000218)
Abnormal external genitalia morphology* (HP: 0000811)		clitoral hypertrophy (HP: 0008665)		hypospadias (HP: 0000047), bilateral cryptorchidism (HP: 0008689)
Atrial septal defect (HP: 0001631)				X
Growth retardation				
Microcephaly* (HP: 0000252)	X	X	X	X
Proportionate short stature* (HP: 0003508)	X	X	X	X
Failure to thrive* (HP: 0001508)	X	X		X
Feeding difficulties* (neonatal) (HP: 0011968)	X	X		
IUGR* (HP: 0001511)		X	X	
Craniofacial findings				
Abnormality of the outer ear* (HP: 0000356)	cupped ear (HP: 0000378)	abnormally folded helix (HP: 0008544)	microtia (HP: 0008551), abnormal earlobe morphology (HP: 0000363)	overfolded helix (HP: 0000396), posteriorly rotated ears (HP: 0000369, HP: 0000358)
Low-set ears (HP: 0000369)	X		X	X

(*Continued on next page*)

Table 1. ***Continued***

	Individual 1	Individual 2	Individual 3	Individual 4
Facial dysmorphism* (HP: 0001999)	large forehead (HP: 0002003), sloping forehead (HP: 0000340), prominent forehead (HP: 0011220), downturned corners of mouth (HP: 0002714), highly arched eyebrow (HP: 0002553), micrognathia (HP: 0000347)	malar flattening (HP: 0000272), wide mouth (HP: 0000154), downslanted palpebral fissures (HP: 0000494), abnormality of the philtrum (HP: 0000288)	ptosis (HP: 0000508)	plagiocephaly (HP: 0001357), prominent forehead (HP: 0011220), highly arched eyebrow (HP: 0002553), synophrys, (HP: 0000664), downslanted palpebral fissures (HP: 0000494), blepharophimosis (HP: 0000581), ptosis (HP: 0000508), long philtrum, (HP: 0000343), thin upper lip vermilion (HP: 000021), micrognathia (HP: 0000347)
Abnormal external nose morphology (HP: 0010938)	abnormal columella morphology (HP: 0009929)	anteverted nares (HP: 0000463)	prominent nasal bridge (HP: 0000426)	prominent nasal bridge (HP: 0000426), prominent nasal tip (HP: 0005274), short columella (HP: 0002000), narrow nares (HP: 0009933)
Epicanthus (HP: 0000286)		X	X	
Abnormal eye physiology* (HP: 0012373)	exotropia (P:0000577), nystagmus (HP: 0000639), astigmatism (HP: 0000483)			
Other				
Abnormality of the musculoskeletal system (HP: 0033127)	lower limb asymmetry (HP: 0100559)	accelerated skeletal maturation (HP: 0005616), abnormal vertebral morphology (HP: 0003468)	hypotonia (HP: 0001252)	
Premature birth* (HP: 0001622)		X	X	
Chronic constipation (HP: 0012450)	X		X	
Apnea (HP: 0002104)			X	X
Gastroesophageal reflux (HP: 0002020)	X			
Hashimoto thyroiditis (HP: 0000872)		X		
Broad-based gait (HP: 0002136)		X		
Thrombocytopenia (HP: 0001873)			X	

Genetic testing and clinical findings with associated HPO terms (see web resources) in individuals 1, 2, and 3, who were homozygous for recurrent homozygous missense variant c.128A>G in *EIF3K* and c.355C>T in *SYNE4*, and individual 4 with the homozygous non-coding *EIF3K* variant c.355-13A>G. The asterisk indicates a feature present in ≥2 individuals in the aggregate cohort of individuals with recurrent homozygous *EIF3K* and *SYNE4* variants who were not available to consent to case-level publication. The ``X" indicates the presence of the clinical finding in that row, and a blank cell indicates that the clinical finding in that row was absent or not assessed. HP/HPO, Human Phenotype Ontology.

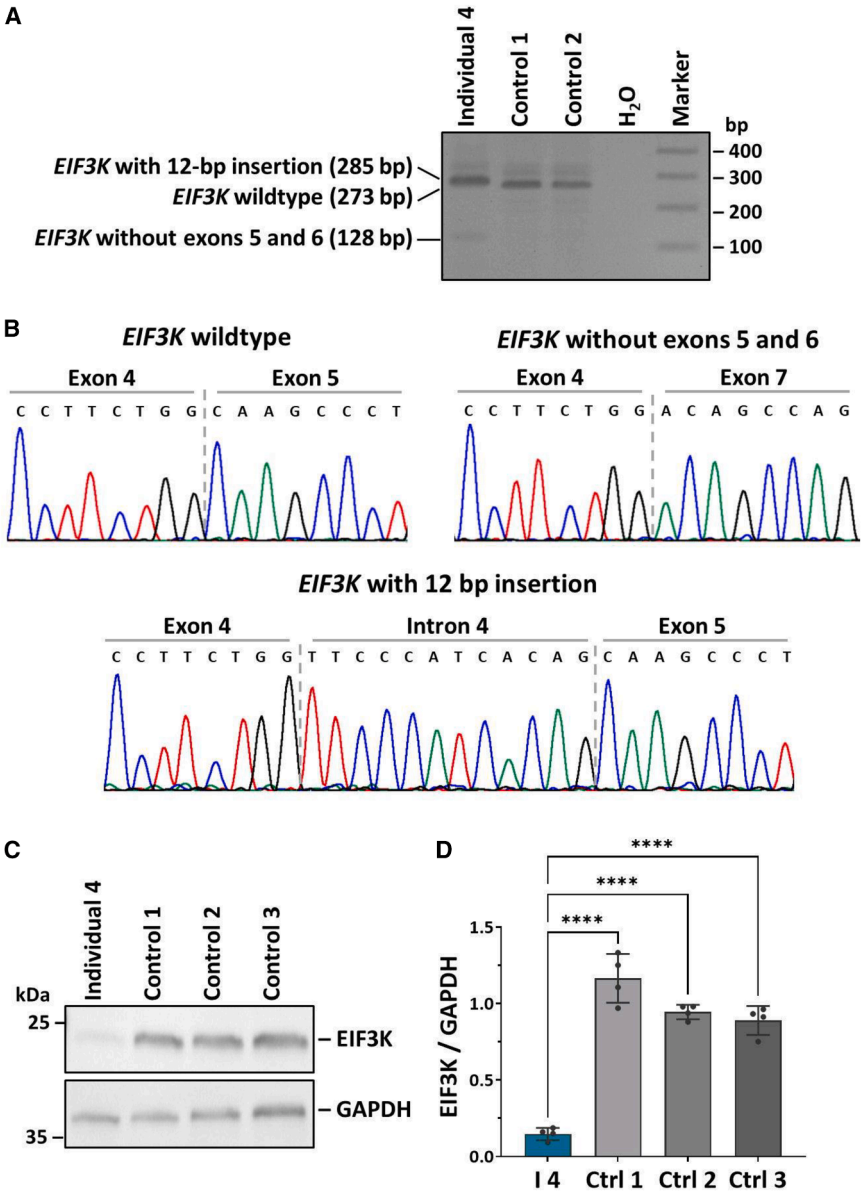

Figure 2. *EIF3K* transcript and protein analysis in fibroblasts from individual 4 with the homozygous c.355-13A>G variant

(A) Agarose gel showing *EIF3K* RT-PCR amplicons generated with primers located in exons 4 and 7 using fibroblast-derived cDNA from individual 4 and two controls. The 273-bp amplicon represents wild-type *EIF3K* transcripts with exon 4 spliced to exon 5 (B, upper left sequence), the 285-bp amplicon represents *EIF3K* transcripts with an insertion of the last 12 bp of intron 4 between exons 4 and 5 (B, lower sequence), and the 128-bp amplicon represents transcripts lacking exons 5 and 6 (B, upper right sequence).

(B) Sequence traces of single-colony PCR products from cloned RT-PCR amplicons of individual 4.

(C) Representative immunoblot of whole-cell lysates obtained from individual 4 and control fibroblasts. Endogenous EIF3K levels were monitored with an anti-EIF3K antibody. An anti-glyceraldehyde 3-phosphate dehydrogenase antibody was used to demonstrate equal loading.

(D) Quantification of EIF3K protein levels. Band intensities of fluorescence signals were quantified using the ChemiDoc imaging system. The mean ± SD of four independent experiments is shown Individual data points are shown. One-way ANOVA with Dunnett's correction was used for statistical analysis. ****, $p \leq 0.0001$; Ctrl, control; I4, individual 4.

is predicted to cause a frameshift and an introduction of a premature stop codon [p.(Gln119Thrfs*4)] (Figure 2B). The data show that the homozygous c.355-13A>G variant causes aberrant splicing of the *EIF3K* pre-mRNA. However, canonically spliced *EIF3K* transcripts are also produced.

Next, we studied whether aberrant splicing influences the EIF3K protein in individual 4's fibroblasts. EIF3K (expected molecular weight of 25 kDa) was detected at a molecular weight of ~23 kDa in control fibroblasts. In individual 4's fibroblasts, we observed a very faint 23-kDa EIF3K band (Figure 2C). Quantification of EIF3K levels revealed a significant reduction to ~15% compared to control fibroblasts (Figure 2D). The remaining EIF3K protein could represent EIF3K wild type and/or mutant [p.(Trp118_Gln119insPheProSerGln)]. Our functional data demonstrate that the homozygous *EIF3K* c.355-13A>G variant caused aberrant splicing and drastically reduced EIF3K protein levels in the fibroblasts of individual 4.

Individual 1

Individual 1 was a nearly 7-year-old Puerto Rican female born full term. She had an echocardiogram after birth, which noted a small patent ductus arteriosus (PDA). She was diagnosed with severe to profound bilateral sensorineural hearing loss (B-SNHL) at <1 year old. Growth retardation was noted with weight, height, and head circumference <1st percentile. She had feeding difficulties, including aspiration of liquids, slow weight gain, failure to thrive, chronic constipation, and gastroesophageal reflux with esophagitis, as well as submucous cleft palate. Dysmorphic craniofacial features were noted and included large, sloping, prominent forehead, micrognathia, low-set, cupped ears, abnormal facial shape, highly arched eyebrows, downturned corners of the mouth, and low-hanging columella. She also had camptodactyly and an adducted thumb. Ocular abnormalities included exotropia, nystagmus, and astigmatism. She had global developmental delay and was nonverbal, with some sign language. Autism was diagnosed at age 2 years, 9 months,

Figure 3. Photographs of individual 4
Facial photographs of individual 4 at 5 weeks (A and B) and 2 years, 6 months (C and D) show a prominent forehead, low-set posteriorly rotated ears with overfolded helices, highly arched eyebrows with synophrys, blepharophimosis, ptosis, downslanted palpebral fissures, a pronounced nasal bridge and tip, narrow nares, short columella, long philtrum, thin upper lip vermillion, and micrognathia. (E and F) At 2 years, 6 months, individual 4 showed camptodactyly of the 2nd–5th fingers (E) and overlapping toe and hypoplastic toenails of the left foot (F).

with details of the diagnostic criteria not available. Around age 4 years, a brain MRI was done and was atypical (Table 1). Brain images were not available for publication.

Individual 2

Individual 2 was an 11-year-old Puerto Rican female born at 36 weeks via induction for intrauterine growth restriction (IUGR) noted at 25 weeks. Individual 2 was diagnosed with severe to profound B-SNHL through newborn screen. Congenital microcephaly and growth retardation were noted at growth parameters <2nd percentile. She spent 6 weeks in a neonatal intensive care unit (NICU) due to poor weight gain. An echocardiogram showed PDA, and the brain MRI showed ventriculomegaly. Dysmorphic craniofacial features included abnormal facial shape, malar flattening, wide mouth, epicanthus, downslanted palpebral fissures, anteverted nares, abnormality of the philtrum, and overfolded helix of the outer ear. Bilateral overlapping toes were noted. She had global developmental delay, intellectual disability, wide-based gait, and was nonverbal, with about 100 communicative signs. She was diagnosed with autism at age 6 (diagnostic criteria not available) and had behavioral concerns including hyperactivity, attention difficulties, impulsivity, and dangerous and self-injurious behaviors. She was found to have advanced bone age and protruding vertebrae in the lumbar spine. Other findings included Hashimoto hypothyroidism and abnormal morphology of the external genitalia (clitoromegaly).

Individual 3

Individual 3 was a 19-year-old Puerto Rican female with a history of nonverbal intellectual disability, dysmorphic craniofacial features, hearing loss, and global developmental delay. The pregnancy was notable for IUGR and premature birth at 31 weeks. She had apnea, hypotonia, microcephaly, and PDA, which required surgery. Moderate to severe SNHL was diagnosed at age 2 years. Head imaging showed thin corpus callosum and unilateral left deficiency of the modiolus and apical turn of the cochlea. She sat at 10 months, walked at 18 months, and had 6 words at age 3 years, when she was referred to genetics, who noted her height and weight <5th percentile and head circumference <3rd percentile. At 8 years of age, she had attention-deficit/hyperactivity disorder (ADHD), mild contracture of the 5th fingers, small toes, ptosis, epicanthal folds, low-set small ears with irregular edge of lobes, prominent nasal bridge, and high palate. Around 10 years of age, she had a seizure with status epilepticus and was hospitalized, but the electroencephalogram did not show any ongoing seizure tendency, so no ongoing anticonvulsants were prescribed. She had a history of behavioral outbursts. Evaluation at age 14 years found chronic constipation, with weight at the 18th percentile and height at the 0 percentile. On a recent visit, low platelets were noted. A paternal aunt had intellectual disability, hearing loss, and unspecified cardiac issues.

Individual 4

Individual 4, a 2-year, 6-month-old male, was the fourth child born to consanguineous healthy Egyptian parents. He had two healthy siblings and one sibling who showed overlapping clinical features but also had additional features of congenital hydrocephalus and refractory epilepsy and passed away at age 14 months. The pregnancy of individual 4 was uncomplicated, and he was delivered at full term by cesarean section, with a low birth weight of 2.5 kg. He was admitted to the NICU for 23 days due to respiratory distress. An echocardiogram at 1 week of age showed PDA and atrial septal defect. Clinical examinations at age 5 weeks and 2.5 years revealed distinctive

craniofacial features, including plagiocephaly, prominent forehead, highly arched eyebrows with synophrys, blepharophimosis, ptosis, and downslanted palpebral fissures (Figures 3A–3D). Additionally, he had low-set, posteriorly rotated ears with overfolded helices, a prominent nasal bridge and tip, narrow nares, a short columella, long philtrum, thin upper lip vermillion, high palate, and micrognathia. He had bilateral camptodactyly of the 2nd–5th fingers, bilateral overlapping toes, hypoplastic toenails (Figures 3E and 3F), bilateral cryptorchidism, and hypospadias. At the age of 2.5 years, growth retardation was noted with weight of 7.5 kg (−3.00 SD), length of 80 cm (−2.70 SD), and head circumference of 42.5 cm (−3.00 SD). He had global developmental delay with partial neck support and spoke only two words, consistent with language delay. Fundoscopy, hearing examination, and brain imaging were normal.

Discussion

The present report suggests that biallelic *EIF3K* variants are associated with an autosomal recessive syndromic neurodevelopmental disorder. All individuals with homozygous *EIF3K* variants showed developmental delays, microcephaly, dysmorphic craniofacial features (Figure 3), digit flexion anomalies, PDA, and genitourinary malformations in males. Nearly all individuals had proportionate short stature and abnormal brain imaging. Our cohort included individuals 1–3, an aggregate cohort of <5 additional Puerto Rican individuals with the recurrent homozygous *EIF3K* missense variant c.128A>G, and individual 4 with the homozygous non-coding variant c.355-13A>G.

There is precedence for autosomal recessive Mendelian disease related to an eIF3 subunit, specifically *EIF3F*, in which biallelic variants cause intellectual developmental disorder 67 (MIM: 618295). *EIF3F*-related neurodevelopmental disorder is characterized by global developmental delay, microcephaly, epilepsy, muscular hypotonia or hypertonia, hearing loss, ophthalmologic anomalies, and short stature.[13,14] Interestingly, a recurrent homozygous missense variant in *EIF3F* has been recognized as a founder variant in 15 families of European/west Asian descent.[14]

All individuals with the recurrent homozygous missense variant c.128A>G in *EIF3K* were homozygous for c.355C>T in *SYNE4*. Nearly all individuals with this haplotype had severe to profound congenital B-SNHL (Figure 2). They were not known to be related to one another, were all of Puerto Rican descent, and the ES did not indicate evidence of consanguinity. This report raises the possibility that the dual homozygosity of these *EIF3K* and *SYNE4* missense variants may lead to the dual diagnosis of neurodevelopmental disorder and hearing loss. A case-level analysis of additional individuals with *EIF3K* variants is needed to determine the gene associated with the hearing loss phenotype.

Statistical analysis within the GeneDx ES database demonstrated that the *EIF3K* c.128A>G and *SYNE4* c.355C>T variants showed LD among affected individuals (Table S2). The co-occurrence of the homozygous variants suggests a potential population founder effect, which has been documented in affected individuals of Puerto Rican descent.[15–17] The early ancestral population of Puerto Rico shows very low genetic diversity, implying an early founder effect that could predate European contact with the island.[18] This linkage analysis provided valuable insight into the rare occurrence of these variants, their relationship to each other, and the increased prevalence of the homozygous pair in affected individuals.

Through GeneMatcher,[12] we also report clinical details of individual 4, harboring the homozygous intronic variant c.355-13A>G in *EIF3K* (Table S1). This proband contributes significantly to the GeneDx cohort with striking phenotypic overlap, disease by variant segregation in his family, and convincing functional evidence that this non-coding variant adversely affects pre-mRNA splicing and drastically reduces EIF3K protein levels in fibroblast cells (Figure 2). While further studies are necessary to prove that partial loss of function is a mechanism of disease for variants in *EIF3K*, the inclusion of individual 4 in this report contributes considerably to potential pathogenicity.

The limitations of our report include only four individuals who consented to case-level publication. There are also limitations to clinical findings, including the 16p11.2 duplication syndrome (MIM# 611913) in individual 1, which could have contributed to her phenotype, lack of detailed audiometric evaluations to know whether the B-SNHL was consistent with the type reported in *SYNE4*, and lack of photographs for the majority of the cohort, making it difficult to determine whether there was a typical facial gestalt.

In summary, we provide initial evidence that biallelic *EIF3K* variants are associated with neurodevelopmental delay, microcephaly, growth retardation, dysmorphic craniofacial features, digit anomalies, cardiac defects, and male genitourinary malformations. Individuals with the recurrent missense c.128A>G *EIF3K* variant shared Puerto Rican ancestry and LD, raising the possibility of a founder effect. Functional studies showed aberrant splicing and significant EIF3K protein reduction for the variant c.355-13A>G, suggesting a potential (partial) loss-of-function mechanism. Our findings support the value of ES, a large clinical laboratory database, and GeneMatcher as important approaches to new gene discovery in undiagnosed and rare diseases.

Data and code availability

ES data were generated during clinical testing; however, study individuals were not consented for data sharing.

Acknowledgments

We gratefully recognize the families who agreed to participate in this project and admire their persistence in working to end their family's diagnostic odyssey. We thank Sina Ramcke for skillful technical assistance. This work was supported by the Deutsche Forschungsgemeinschaft (KU 1240/13-1, to K.K.).

Declaration of interests

B.M., M.J.G.S., H.G., Y.B., A.C., A.E.D., L.M.D., L.B.H., K.G.M., O. L.R., A.R., and I.M.W. are employees of and may own stock in GeneDx, LLC.

Supplemental information

Supplemental information can be found online at https://doi.org/10.1016/j.xhgg.2025.100438.

Web resources

Human Phenotype Ontology (HPO): https://hpo.jax.org/
Online Mendelian Inheritance in Man (MIM): http://www.omim.org/
UniProt: https://www.uniprot.org/uniprotkb/Q9UBQ5/entry#family_and_domains

Received: February 10, 2025
Accepted: April 8, 2025

References

1. Mayeur, G.L., Fraser, C.S., Peiretti, F., Block, K.L., and Hershey, J.W.B. (2003). Characterization of eIF3k: a newly discovered subunit of mammalian translation initiation factor eIF3. Eur. J. Biochem. *270*, 4133–4139.
2. Yin, Y., Long, J., Sun, Y., Li, H., Jiang, E., Zeng, C., and Zhu, W. (2018). The function and clinical significance of eIF3 in cancer. Gene *673*, 130–133.
3. Wei, Z., Zhang, P., Zhou, Z., Cheng, Z., Wan, M., and Gong, W. (2004). Crystal structure of human eIF3k, the first structure of eIF3 subunits. J. Biol. Chem. *279*, 34983–34990.
4. Masutani, M., Sonenberg, N., Yokoyama, S., and Imataka, H. (2007). Reconstitution reveals the functional core of mammalian eIF3. EMBO J. *26*, 3373–3383.
5. Chen, Y., Cao, B., Zheng, W., Sun, Y., and Xu, T. (2022). eIF3k inhibits NF-κB signaling by targeting MyD88 for ATG5-mediated autophagic degradation in teleost fish. J. Biol. Chem. *298*, 101730.
6. Cattie, D.J., Richardson, C.E., Reddy, K.C., Ness-Cohn, E.M., Droste, R., Thompson, M.K., Gilbert, W.V., and Kim, D.H. (2016). Mutations in Nonessential eIF3k and eIF3l Genes Confer Lifespan Extension and Enhanced Resistance to ER Stress in Caenorhabditis elegans. PLoS Genet. *12*, e1006326.
7. Lin, Y.M., Chen, Y.R., Lin, J.R., Wang, W.J., Inoko, A., Inagaki, M., Wu, Y.C., and Chen, R.H. (2008). eIF3k regulates apoptosis in epithelial cells by releasing caspase 3 from keratin-containing inclusions. J. Cell Sci. *121*, 2382–2393.
8. Tomasoni, M., Beyeler, M.J., Vela, S.O., Mounier, N., Porcu, E., Corre, T., Krefl, D., Button, A.L., Abouzeid, H., Lazaros, K., et al. (2023). Genome-wide Association Studies of Retinal Vessel Tortuosity Identify Numerous Novel Loci Revealing Genes and Pathways Associated With Ocular and Cardiometabolic Diseases. Ophthalmol. Sci. *3*, 100288.
9. Khan, U., Habibur Rahman, M., Salauddin Khan, M., Hossain, M.S., and Morsaline Billah, M. (2022). Bioinformatics and network-based approaches for determining pathways, signature molecules, and drug substances connected to genetic basis of schizophrenia etiology. Brain Res. *1785*, 147889.
10. Fu, J.M., Satterstrom, F.K., Peng, M., Brand, H., Collins, R.L., Dong, S., Wamsley, B., Klei, L., Wang, L., Hao, S.P., et al. (2022). Rare coding variation provides insight into the genetic architecture and phenotypic context of autism. Nat. Genet. *54*, 1320–1331.
11. Zhou, X., Feliciano, P., Shu, C., Wang, T., Astrovskaya, I., Hall, J.B., Obiajulu, J.U., Wright, J.R., Murali, S.C., Xu, S.X., et al. (2022). Integrating *de novo* and inherited variants in 42,607 autism cases identifies mutations in new moderate-risk genes. Nat. Genet. *54*, 1305–1319.
12. Sobreira, N., Schiettecatte, F., Valle, D., and Hamosh, A. (2015). GeneMatcher: a matching tool for connecting investigators with an interest in the same gene. Hum. Mutat. *36*, 928–930.
13. Martin, H.C., Jones, W.D., McIntyre, R., Sanchez-Andrade, G., Sanderson, M., Stephenson, J.D., Jones, C.P., Handsaker, J., Gallone, G., Bruntraeger, M., et al. (2018). Quantifying the contribution of recessive coding variation to developmental disorders. Science *362*, 1161–1164.
14. Hüffmeier, U., Kraus, C., Reuter, M.S., Uebe, S., Abbott, M.A., Ahmed, S.A., Rawson, K.L., Barr, E., Li, H., Bruel, A.L., et al. (2021). EIF3F-related neurodevelopmental disorder: refining the phenotypic and expanding the molecular spectrum. Orphanet J. Rare Dis. *16*, 136.
15. De Jesús-Rojas, W., Muñiz-Hernández, J., Alvarado-Huerta, F., Meléndez-Montañez, J.M., Santos-López, A.J., and Mosquera, R.A. (2022). The Genetics of Primary Ciliary Dyskinesia in Puerto Rico. Diagnostics *12*, 1127.
16. Al-Zaidy, S.A., Malik, V., Kneile, K., Rosales, X.Q., Gomez, A. M., Lewis, S., Hashimoto, S., Gastier-Foster, J., Kang, P., Darras, B., et al. (2015). A slowly progressive form of limb-girdle muscular dystrophy type 2C associated with founder mutation in the SGCG gene in Puerto Rican Hispanics. Mol. Genet. Genomic Med. *3*, 92–98.
17. Gonzaga-Jauregui, C., Gamble, C.N., Yuan, B., Penney, S., Jhangiani, S., Muzny, D.M., Gibbs, R.A., Lupski, J.R., and Hecht, J.T. (2015). Mutations in COL27A1 cause Steel syndrome and suggest a founder mutation effect in the Puerto Rican population. Eur. J. Hum. Genet. *23*, 342–346.
18. Martínez-Cruzado, J.C., Toro-Labrador, G., Viera-Vera, J., Rivera-Vega, M.Y., Startek, J., Latorre-Esteves, M., Román-Colón, A., Rivera-Torres, R., Navarro-Millán, I.Y., Gómez-Sánchez, E., et al. (2005). Reconstructing the population history of Puerto Rico by means of mtDNA phylogeographic analysis. Am. J. Phys. Anthropol. *128*, 131–155.